Vision Research 217 (2024) 108367

Contents lists available at ScienceDirect

Vision Research

journal homepage: www.elsevier.com/locate/visres

Secondary not subordinate: Opsin localization suggests possibility for color sensitivity in salticid secondary eyes

Mireille Steck [a,*], Sophia J. Hanscom [a], Tom Iwanicki [a,b], Jenny Y. Sung [c], David Outomuro [c,d], Nathan I. Morehouse [c], Megan L. Porter [a]

[a] University of Hawai'i at Mānoa, Honolulu HI 96822 USA
[b] The Earth Commons Institute, Georgetown University, Washington DC 20057 USA
[c] University of Cincinnati, Cincinnati OH 45221
[d] University of Pittsburgh, Pittsburgh PA 15260 USA

ARTICLE INFO

Keywords:
Salticidae
Opsin
Secondary eyes
Color vision

ABSTRACT

The principal eyes of jumping spiders (Salticidae) integrate a dual-lens system, a tiered retinal matrix with multiple photoreceptor classes and muscular control of retinal movements to form high resolution images, extract color information, and dynamically evaluate visual scenes. While much work has been done to characterize these more complex principal anterior eyes, little work has investigated the three other pairs of simpler secondary eyes: the anterior lateral eye pair and two posterior (lateral and median) pairs of eyes. We investigated the opsin protein component of visual pigments in the eyes of three species of salticid using transcriptomics and immunohistochemistry. Based on characterization and localization of a set of three conserved opsins (*Rh1* - green sensitive, *Rh2* - blue sensitive, and *Rh3* - ultraviolet sensitive) we have identified potential photoreceptors for blue light detection in the eyes of two out of three species: *Menemerus bivittatus* (Chrysillini) and *Habrocestum africanum* (Hasarinii). Additionally, the photoreceptor diversity of the secondary eyes exhibits more variation than previous estimates, particularly for the small, posterior median eyes previously considered vestigial in some species. In all three species investigated the lateral eyes were dominated by green-sensitive visual pigments (RH1 opsins), while the posterior median retinas were dominated by opsins forming short-wavelength sensitive visual pigments (e.g. RH2 and/or RH3/RH4). There was also variation among secondary eye types and among species in the distribution of opsins in retinal photoreceptors, particularly for the putatively blue-sensitive visual pigment formed from RH2. Our findings suggest secondary eyes have the potential for color vision, with observed differences between species likely associated with different ecologies and visual tasks.

1. Introduction

The family Salticidae, also known as 'jumping spiders' for their active, visually guided, predatory lifetyle, is one of the most diverse families of modern spiders where all species are known for being highly visual predators (Land, 1985; Hill and Richman, 2009; Foelix, 2011; Cerveira et al., 2019; Morehouse, 2020). Similar to most species of spiders, salticids have four pairs of eyes named for their position around the circumference of the head: the single pair of 'principal' or anterior median eyes (AMEs); and the three pairs of 'secondary eyes' comprised of the anterior lateral (ALEs), posterior median (PMEs), and posterior lateral (PLEs) eyes (Fig. 1). Studies of jumping spider vision have predominately focused on their large forward facing principal eyes (see Winsor et al., 2023 for review), which form extraordinarily high resolution images via a dual-lens system while dynamically evaluating visual scenes thanks to muscular guidance of retinal position within the head (Land 1969a, b; Blest and Price, 1984; Nagata et al., 2012). The principal eyes also make use of input from tiered photoreceptors, and sometimes filters, to achieve color vision (Blest, Hardie, McIntyre, & Williams, 1981; Blest & Price, 1984; Blest & Sigmund, 1984; Blest, 1985a; Blest, 1985b; Blest, O'Carroll, & Carter, 1990; Nagata, Koyanagi, & Tsukamoto, 2012; Zurek, Cronin, & Taylor, 2015; Morehouse, Buschbeck, & Zurek, 2017) and depth perception (Nagata et al., 2012). In contrast, much less is known about the visual function and spectral sensitivity of the secondary eyes.

Based on early anatomical work in the group, the ultrastructure of

* Corresponding author.
E-mail address: steck4@hawaii.edu (M. Steck).

https://doi.org/10.1016/j.visres.2024.108367
Received 7 December 2023; Received in revised form 29 January 2024; Accepted 13 February 2024

the principal (AME) and secondary (ALE, PME, PLE) eyes in jumping spiders is drastically different, with the AMEs having an everted photoreceptor arrangement (i.e. rhabdoms distal to the cell body) and the secondary eyes having an inverted arrangement (i.e. cell body distal to the rhabdoms; Blest 1983; Land 1985). Aside from eye arrangement, the two eye types also have different shapes and mobility: principal eyes have unique, boomerang-shaped, mobile retinas which can move independently of one another thanks to a dedicated set of retinal muscles (Land 1969a; Richman and Jackson, 1992; Dolev, 2016; Morehouse, 2020), while secondary eyes are fixed retinal cups. Even the function of the two eye types differs drastically, with the principal eyes used in spatial resolution, depth perception, and color vision (Land 1969a; Nagata et al., 2012; Zurek et al., 2015; Dolev, 2016; Cerveira et al., 2019), compared to the simple motion detection and basic shape perception performed by the secondary eyes (Land, 1969a,1985; Duelli, 1978; Blest, 1983; Harland, 2000; Bednarski et al., 2012; Zurek et al., 2010; Spano et al., 2012; Jakob et al., 2018). Moreover, the ultrastructure of the secondary eyes has been investigated in only a few salticid species (tribes/subfamilies: Plexippini, Euophryini, Dendryphantini, Spartaeinae, and Lyssomaninae; Eakin and Brandenburger, 1971; Yamashita and Tateda, 1976; Duelli, 1978; Hardie and Duelli, 1978; Blest, 1987). Despite these studies finding little variation among photoreceptor arrangements in retinal mosaics, secondary eye types (e.g. ALE vs. PME vs. PLE) vary in size, position, and fields of view when compared within an individual and among taxa (Land, 1985). This variation in secondary eye placement and morphology hints at the potential for differences in underlying photoreceptor arrangements and visual functions that have yet to be characterized.

In the few salticid species where the secondary eyes have been studied, the uniform retinal mosaic of these eyes is formed by a photoreceptor cell surrounded by transparent glial cells and pigmented screening cells; the support cells are often in the configuration of a square or six-pointed star mosaic (Eakin & Brandenburger, 1971; Blest, 1983, 1987). In contrast, the retinal mosaic in principal eyes can be quite diverse, with one to four rhabdomeres per photoreceptive cell that vary in structure based on location in the retina (e.g. tiers 1–4) and by

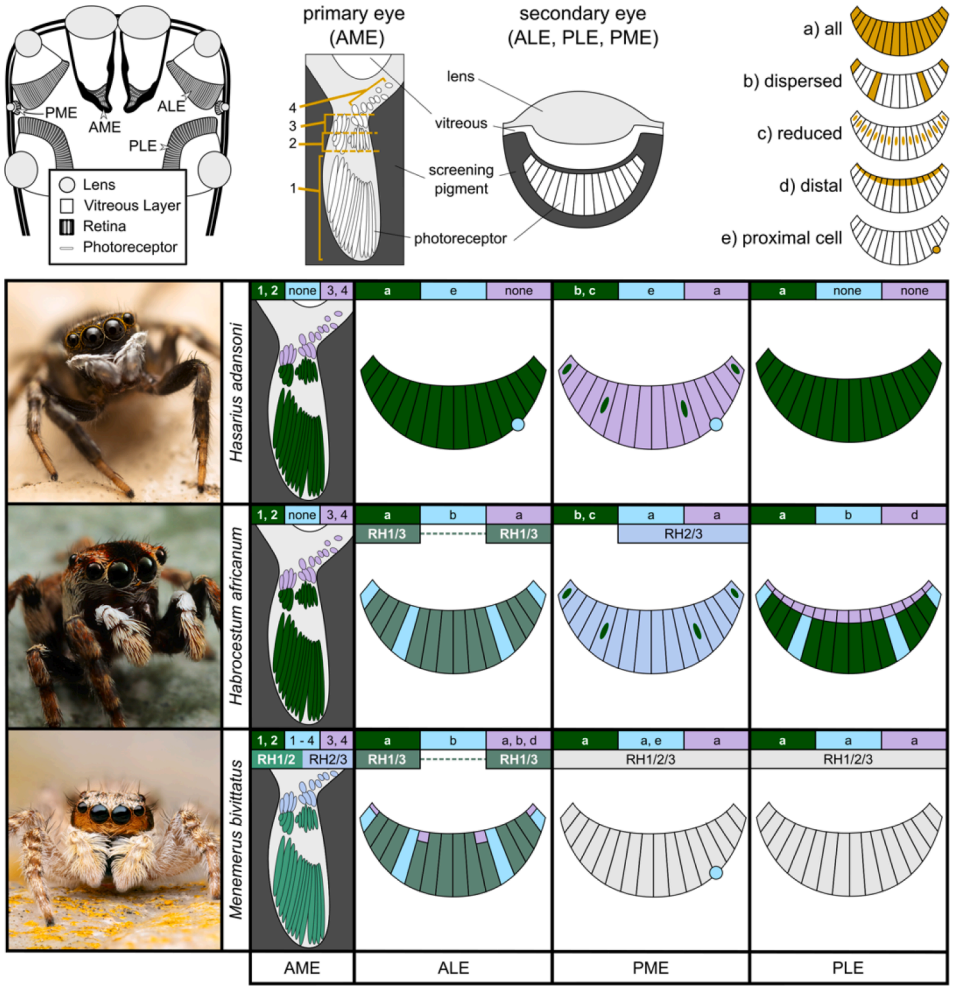

Fig. 1. Top left - diagram of a cross section of a salticid cephalothorax representing placement and structure of eyes: lenses in gray circles, vitreous outlined with a black line, and retinas (black) lined with photoreceptors in approximate orientations (white). Top center - diagrams of primary retinas (left) with tier (1–4) orientation labeled and secondary eye anatomy (right). Top right - diagrams of immunohistochemistry labeling patterns (a-e) observed in secondary eyes. Where protein localization occurs, areas in the retina are highlighted in yellow for a) all photoreceptors, b) dispersed photoreceptors, c) reduced photoreceptors, d) distal cells or photoreceptors, and e) proximal cells external to photoreceptors. Bottom - a summary diagram of immunohistochemistry results for each species studied shown in one row from left to right: an image of the animal, species name, and diagrams for the AME retina, ALE retina, PME retina, and PLE retina. Diagrams illustrate localization patterns for RH1 (green), RH2 (blue), and RH3/RH4 (purple) opsins. Letters above each retina diagram describe the labeling patterns of each opsin based on tiers 1–4 in the AME retinas or on panels a-e in the secondary eyes (ALE, PME, and PLE retinas). Where multiple opsins localize across the entire retina, associated colors are overlapped with secondary boxes to annotate which proteins share patterns. Photo credit: *H. adansoni* (Austin Greene); *H. africanum* (Wynand Uys); and *M. bivittatus* (Vida van der Walt). (For interpretation of the references to color in this figure legend, the reader is referred to the web version of this article.)

taxa (Eakin & Brandenburger, 1971; Blest, 1983; Blest & Price, 1984; Blest & Sigmund, 1984; Blest, 1985; Blest, O'Carroll, & Carter, 1990). The photoreceptors are suspended in an optically transparent matrix with screening cells surrounding the photoreceptor bodies distal to the photoreceptive units (Eakin & Brandenburger, 1971; Blest, 1983; Blest & Price, 1984; Blest & Sigmund, 1984; Blest, 1985; Blest, O'Carroll, & Carter, 1990). Spectral sensitivities also vary across eyes; in the principal eyes, ultraviolet (UV) and green sensitivity are prevalent with expanded sensitivities documented in some species (Land 1969b; De Voe, 1975; Yamashita and Tateda, 1976; Blest et al., 1981; Zurek et al., 2015; Glenszczyk et al., 2022), while the secondary eyes have only been found to have green sensitivity (Yamashita and Tateda, 1976; Hardie and Duelli, 1978). Spectral sensitivities are most commonly determined by peak absorbance of the associated visual pigment(s), composed of an opsin protein tethered to a vitamin-A-derived chromophore. Opsin proteins are an integral part of vision, forming the visual pigments that absorb specific wavelengths of light and transduce a signal to the brain. Investigation of the diversity of opsin expression within and across eyes therefore provides an understanding of the foundation for light detection, as well as insights into the potential color detection abilities of each eye type.

Despite a long history of anatomical studies of salticid AMEs, the first molecular characterization of opsins from within the group was more recent (Koyanagi et al., 2008) and is still limited to only a few species. In 2008, Koyanagi *et al.* characterized opsins from two species of jumping spiders: *Plexippus paykulli* (Plexippina) and *Hasarius adansoni* (Hasariini). Subsequent molecular characterizations focused on the species *H. adansoni* and demonstrated the expression of four opsin genes across the eight eyes: a green-sensitive opsin (*Rh1*); a blue-sensitive opsin (*Rh2*); and two UV-sensitive opsins (*Rh3* and *Rh4*) (Koyanagi et al., 2008; Nagata et al., 2012; Terakita and Nagata, 2014). Based on RT-PCR, *in situ* hybridization (Nagata et al., 2012), and immunohistochemistry (Terakita and Nagata, 2014) studies, these four opsins were shown to have distinct expression patterns in each eye type. Almost all of the eyes in *H. adansoni* utilize two opsins, though the combinations differ by eye type (Table 1).

While *H. adansoni* is the only species of jumping spider where eyes have been investigated across multiple levels of biological organization, including opsin transcript expression, protein localization patterns, and photoreceptor spectral sensitivities (Nagata et al. 2012; Terakita and Nagata 2014), none of the previous studies in this species presented a comprehensive look at the localization patterns of all four opsins across all four pairs of eyes. The presence of the putatively blue-sensitive *Rh2* only in the *H. adansoni* posterior eyes (e.g. PME, PLE) and not the secondary ALEs also hints at functional diversity between the secondary eyes more broadly (Table 1). Furthermore, the paucity of opsin data across species leaves open questions regarding the mechanisms behind the expanded sets of spectral sensitivities documented in some species (Yamashita and Tateda, 1976; Glenszczyk et al., 2022). In this study, we begin elucidating the diversity of form and function in jumping spider eyes by characterizing the diversity of expressed visual opsins and their protein localization patterns across all four pairs of eyes in three species of salticids from two closely related tribes: *Hasarius adansoni* and *Habrocestum africanum* (Hasariini), and *Menemerus bivittatus* (Chrysillini). These results build a foundation for understanding the potential for color vision both across eye types within a species and among species.

Table 1
Summary of evidence for opsin transcript expression and protein localization in *Hasarius adansoni* eyes from published studies (Nagata et al., 2012; Terakita & Nagata, 2014) versus results from this study. Evidence for opsin in each retina (i.e., AME, ALE, PME, PLE) and/or tier (i.e., AME T1-T4): / = data from RT-PCR; × = data from RT-PCR and ISH; ⊙ = data from IHC; ⊘ = evidence from RT-PCR and IHC; ⊗ = evidence from RT-PCR, ISH, and IHC.

		OPSIN RETINAL DISTRIBUTION PATTERNS						
		(Nagata 2012; Terakita 2014)				(This Study)		
		Rh1	**Rh2**	**Rh3**	**Rh4**	**Rh1**	**Rh2**	**Rh3/Rh4**
AME	T1	⊗				⊙		
	T2	⊗				⊙		
	T3			⊗				⊙
	T4			⊗				⊙
ALE		⊘				⊙	⊙	
PME			⊗		⊗	⊙	⊙	⊙
PLE		⊘	×		/	⊙		

2. Methods & materials

2.1. Specimen collection and preservation

Adult male and female *Hasarius adansoni* (tribe Hasariini) were collected from Mānoa Cliffs Trail in dry leaf litter (March 2022; Hawai'i DLNR permit I3028), and *Menemerus bivittatus* (tribe Chrysillini) specimens were collected from walls and eucalyptus trees at the University of Hawai'i at Mānoa (no permit necessary); both species were fixed within 24 h of collection. Adult *Habrocestum africanum* (tribe Hasariini) were collected in South Africa (Ezemvelo KZN Wildlife permit OP 3923/2019) and kept at 24 °C and 55 % RH under 12 hr light:dark cycles at the University of Cincinnati until preservation 4 months later (December 2019 - February 2020). Entire cephalothoraxes were dissected from the abdomen, and legs were removed prior to preservation. Specimens were preserved in RNAlater (Thermo Fisher Scientific) for use in transcriptomics and opsin confirmation using Reverse Transcriptase Polymerase Chain Reactions (RT-PCR; see Supplemental Methods). Specimens preserved for immunohistochemistry (IHC) were preserved in 4 % paraformaldehyde in phosphate buffered saline (PBS) and transferred to PBS after one day of fixation. Prior to histological sectioning, these specimens were bisected horizontally (across the cephalothorax to remove extra muscle tissue) and coronally below the anterior median eyes (to separate the dorsal and ventral carapace) to allow for complete perfusion of the paraffin wax.

2.2. Transcriptomes

Total RNA was extracted from one male and one female of each species using an RNeasy Mini Kit (Qiagen, USA) according to the manufacturer's suggestions for RNAlater preservation, using on-column DNAse digestion. Between 1 and 2 μg of total RNA was obtained from adult cephalothoraxes and up to 1 μg of RNA was sequenced at Novogene Corporation Inc. (Sacramento, CA, USA) using a poly-A tail enrichment kit on a shared Novaseq 6000 PE150 lane to obtain approximately 50 million paired reads per individual. Raw reads were trimmed using Trim Galore (0.6.5; Babraham Bioinformatics) to remove terminal Ns and sequences below a phred score of 33. Three assemblies were made per species: one male, one female, and one pooled, using default parameters with Trinity (v.2.6.6; Grabherr et al., 2011). The three assemblies were then combined per species and redundant contigs, low quality coding sequences, and isoforms or paralogs were filtered out using the euGene/EvidentialGene tr2caads4.pl script (13-Jan-2022; Gilbert, 2019). Assembly completeness was tested using Benchmarking Universal Single-Copy Ortholog (BUSCO) assessment as implemented on galaxy.eu against the arachnid database (v10; Manni et al., 2021). Newly generated RNA-seq raw read datasets are available on NCBI's Sequence Read Archive (SRA) database under BioProject PRJNA1068112.

Transcriptomes were searched for visual opsins using published *Hasarius adansoni Rh1–4* mRNA sequences, and non-visual opsins published from the wandering spider, *Cupiennius salei* (AB251846, AB251847, AB251848, AB506462, HF566406, HF566407, HF566408) using tBLASTx, with a maximum of 25 hits, and max e-value of $1e^{-5}$ implemented in Geneious software (USA). Resulting opsin hits were reciprocal blasted using blastx against the standard non-redundant nucleotide database available from the National Center for

Biotechnology Information (NCBI) using a maximum of 10 target sequences to confirm opsin identification. Any contigs not resulting in arthropod opsin hits were removed from the dataset. Because fragments can result in spurious identities when using BLAST, and multiple instances of ultraviolet-sensitive-like opsins were identified, a MAFFT alignment (G-INS-i, using legacy gap penalty, v7.450; Katoh et al., 2002; Katoh and Standley, 2013) of resulting opsin hits was created using insect *Drosophila melanogaster* rhodopsins (Rh1-7) and all opsins from *Cuppienius salei* (Araneae; Trechalidae) as references for opsin clade identity. Two additional transcriptome assemblies were generated, as above, from public data (Bioprojects PRJNA277111 and PRJNA254752) to investigate the opsin repertoire of a closely related family of non-web-building, ambush-predating spiders (Araneae: Lycosidae: *Pardosa pseudoannulata* and *Schizocosa rovneri*). To root the opsin phylogeny, a subset of Placozoa (*Trichoplax* sp. H2) opsin proteins and two closely related GPCRs (RDD42723, RDD42726, RDD42729, RDD42730, RDD42744, RDD42745, RDD37788, RDD39576) were chosen based on previous phylogenies (Porter et al., 2012; Ramirez et al., 2016; Gühmann et al., 2022). The final protein alignment was trimmed to ensure 90 % of the sequences included data, and a phylogenetic tree was generated using IQtree inference using automatic substitution model determination and ultrafast bootstrap analysis (1000 replicates; Trifinopoulos et al., 2016). The consensus tree was viewed, rooted, and refined using FigTree software (v1.4.4; Rambaut, 2018).

2.3. Immunohistochemistry

Three polyclonal antibodies designed to recognize RH1, RH2, and UVS (i.e. both RH3 and RH4) opsin proteins were purified from rabbits (ABclonal, USA) using Nagata et al., 2012 epitopes; compatibility of the epitope was confirmed using sequence comparisons against *M. bivittatus* and *H. africanum* opsin contigs prior to labeling (Table 2). While the UVS antibody does not differentiate between the RH3 and RH4 opsins in *H. adansoni*, only RH3 was identified from *M. bivittatus* and *H. africanum* transcriptomes and therefore this antibody is predicted to only label RH3 in these species.

Specimens were embedded in paraffin wax and cut into 5 μm sections at the Histopathology Core at the John A. Burns School of Medicine, taking care to position the specimens so the blade would cut coronally from the posterior to the anterior side of the animal to prevent shearing of the tissue. Specimens were also sectioned dorsal to ventral in order to capture the posterior median eyes (PMEs) before the specimen separated from the wax. Six individuals for *Hasarius adansoni* were tested (3 male, 3 female); five individuals for *Menemerus bivittatus* (2 female, 3 male), and three individuals for *Habrocestum africanum* (3 female). For each species, opsin localization patterns in each set of eyes were confirmed in at least two individuals, with the most intact retinal tissue used for final imaging.

Sections were deparaffinized using a series of 3 min washes: 100 % xylene twice, 50 % xylene: 50 % ethanol, 100 % ethanol twice, 95 %, 70 %, and 50 % ethanol before final incubation in cold running water. Tissue permeation was done in PBS with 0.1 % Triton X-100 (PBS-Tx) for 10 min three times. To block nonspecific binding sites, sections were incubated in humidified hybridization chambers with puddled 10 % normal goat serum (NGS) at room temperature for 2 h (Thermo Fisher Scientific). Primary antibodies were diluted using between 2 and 40 μg per mL PBS-Tx and puddled onto slides to incubate in hybridization chambers for one hour. Following the incubation slides were washed in PBS-Tx three times for 10 min each. Secondary antibodies (DyLight 594 goat anti-rabbit IgG, Invitrogen) were diluted with PBS-Tx (5:1000 or 1:100). Slides were incubated for one hour in dark hybridization chambers. Three final washes in PBS-Tx, for 10 min each, were performed prior to mounting samples in ProLong™ Gold Antifade Mountant with DAPI (Invitrogen). Negative controls were prepared by replacing the primary antibodies with PBS-Tx and using mounting media with ProLong™ Gold Antifade Mountant without DAPI (Invitrogen). Imaging was performed at the Biological Electron Microscope Facility (University of Hawai'i at Mānoa) using a Leica confocal laser microscope (TCS SP8 X). For confirmation of patterns observed by Nagata et al. (2012), single images were taken in the brightest plane for *H. adansoni,* whereas maximum-projection images were generated from z-stacks for *H. africanum* and *M. bivittatus* to capture more complete cell

Table 2
Comparison of *Hasarius adansoni* opsin epitopes (anti-RH1, anti-RH2, anti-RH3/4) with visual opsins for *Habrocestum africanum* and *Menemerus bivittatus*. Alignments of *H. adansoni* epitopes with *H. africanum* and *M. bivittatus* RH1-RH3 opsins show the similarity (%) for the aligned region. For each sequence, identical bases (.), gaps (-), or amino acid changes (alphabetic one letter codes) are depicted, with color coding to indicate hydrophobicity (black), charged (orange), or uncharged (blue) amino acids; underlined amino acids indicate difference in property from the epitope.

H. adansoni anti-RH1		GISHPKYRAALHDKFPCLKCGSDSPKGDSASTVA-ESEKAGE	
H. africanum	RH1	.....D....	**97.6%**
	RH2	..........FQ...SFA.TTE.DVV.NK.E.TLVTDEKPP	45.2%
	RH3	AL...R..LE.QN.L.W.CINEKAEASGP.DDSVSKTTEHVA	23.8%
M. bivittatus	RH1	.....N.A.E.....S.AD.G..	**83.3%**
	RH2	..........FQ...S.A.TTETEVV.NK.E.TLVTDEKPP	45.2%
	RH3	AI...R..LE.QTRL.W.CINEKAETSGP.DDSVSKTTEHVA	21.4%
H. adansoni anti-RH2		GISHPKYRAALFEKFPSLACTTESDVTDNKSEVTLVTDEKPPKTQEA	
H. africanum	RH1	..........HD...CLK.GSD.PKG.SA.T.A-ES.KAGE-----	42.6%
	RH2	..........Q....F........V.....	**93.6%**
	RH3	AL...R..LE.QN.L.W.CINEKAEASGPADDSVSK.T.HVA-----	23.4%
M. bivittatus	RH1	..........HD...C.N.AS..PKG.SA.T.ASEA.KGGE-----	46.8%
	RH2	..........Q.....TE.V.....	**91.5%**
	RH3	A....R..LE.QTRL.W.CINEKAETSGPADDSVSK.T.HVA-----	34.0%
H. adansoni anti-RH3/4		ALSHPRYRLELQNKLPWLCINEKAEASGPADDSISKTTECAA	
H. africanum	RH1	GI...K..AA.HD.F.C.KCGSDSPKGDS.STVA-ESDKAGE	23.8%
	RH2	GI...K..AA.FQ.F.SFACTTESDVVDNKSEVTLVTDEKPP	23.8%
	RH3	.....V.....HV.	**92.9%**
M. bivittatus	RH1	GI...K..AA.HD.F.C.NCASESPKGDS.STVA.EADKGGE	26.2%
	RH2	GI...K..AA.FQ.F.S.ACTTET.VVDNKSEVTLV.D.KPP	28.6%
	RH3	.I.....TR.....T.....V.....HV.	**83.3%**

structure. All final images were corrected to the same luminance levels (minimum and maximum) as the tissue of negative controls.

3. Results & discussion

3.1. Salticid visual systems transcribe three opsins

All of the species investigated expressed a conserved set of three rhabdomeric opsins (*Rh1-3*), with gene duplication in only two lineages: the previously identified *Rh3/Rh4* duplication in the salticid *H. adansoni* (Nagata et al., 2012), and an *Rh2* duplication in the lycosid *S. rovneri* (Fig. 2, Table 3). In the studied salticids, *Rh1* had the highest expression levels, followed by *Rh2* (*Hasarius* and *Habrocestum*) or *Rh3* (*Menemerus*). In contrast, the lycosids predominantly expressed *Rh2*, followed by *Rh1*, then *Rh3* (Fig. 2), potentially indicating a shift in opsin usage between these two families due to ecological or environmental differences. Additionally, the expression levels of *Rh2* in *H. africanum* suggests the first recorded potential sexual dimorphism in opsin expression in spiders, with males expressing much higher levels than females. However, we were not able to further investigate this possibility as we only had adult females available for immunohistochemical studies. Four types of non-visual opsins also were identified from salticids: pteropsin, peropsin, arthropsin and *Rh7*, while in the lycosids we only detected pteropsin and/or peropsin (Fig. 2). All newly identified opsin sequences grouped with published opsins from the wandering spider, *Cuppienius salei* (Trechaleidae), supporting their identity, with the exception of *Rh7*, which has not been previously identified from a spider (Fig. 2). The confirmation of a conserved set of three rhabdomeric opsins with relatively high expression values (>10 TPM) in salticid cephalothorax transcriptomes suggests that *Rh1-3* are likely involved in visual processes, and were therefore targeted for immunohistochemical studies of salticid eyes.

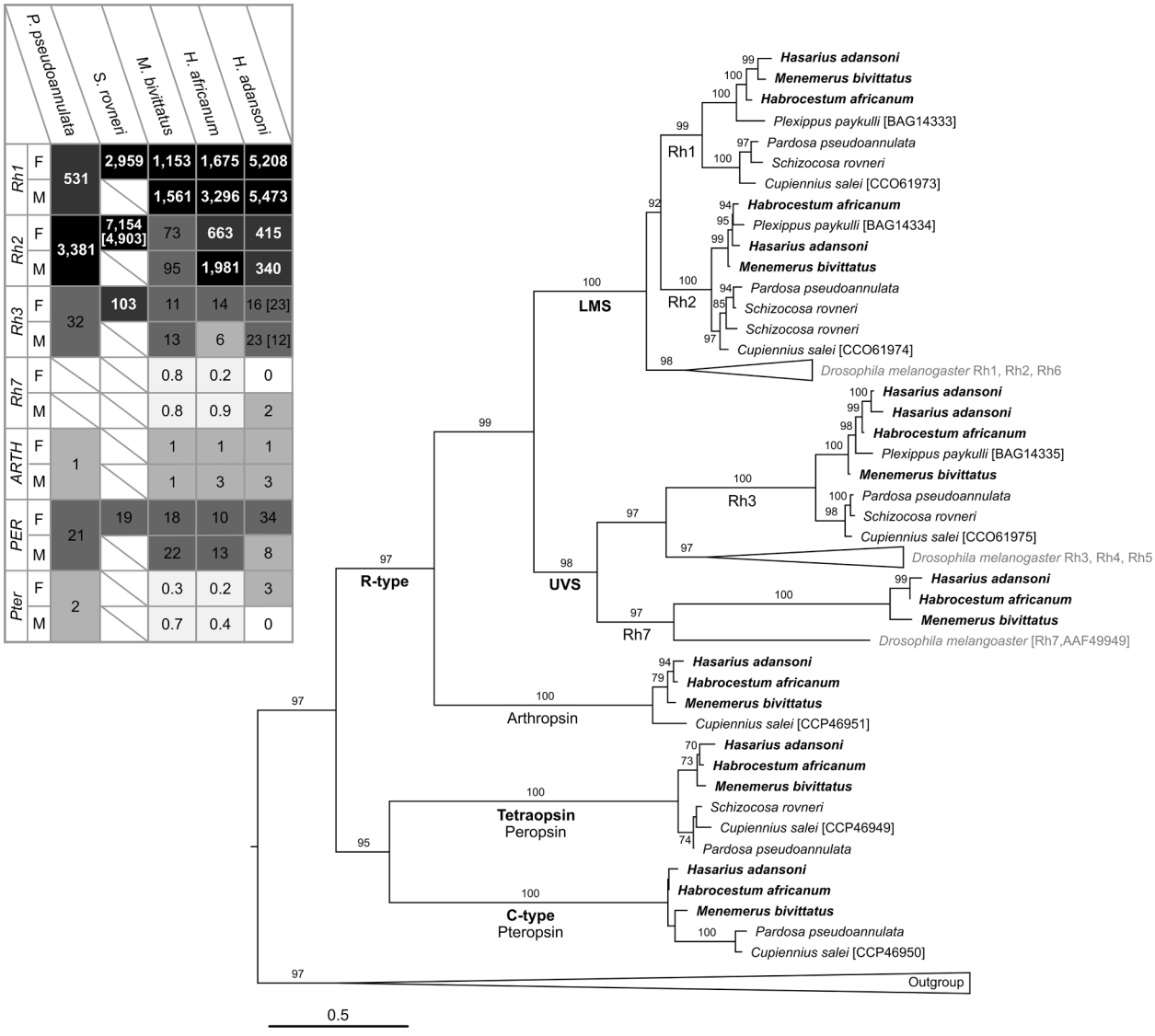

Fig. 2. Maximum likelihood tree of salticid opsins identified in this study, including opsins from three additional spider species - *Pardosa pseudoannulata* and *Schizocosa rovneri* (Lycosidae) and *Cupiennius salei* (Trechaleidae) - and the dipteran fly *Drosophila melanogaster* for reference. Based on the reference sequences, previously defined opsin evolutionary lineages are labeled on the corresponding branches. The numbers above the branches represent bootstrap support values. The heatmap in the upper left corner displays the expression levels of each identified opsin from both a male and a female individual of each salticid species; the sex of the lycosid *P. pseudoannulata* individual used for sequencing was not specified and therefore is represented as a single box for each opsin (with expression of duplicated genes represented in brackets [] for *H. adansoni Rh3/[Rh4]* and *S. rovneri Rh2* duplicates). Darker boxes represent higher levels of expression (color change occurs on a logarithmic scale), while a diagonal line through a box indicates that opsin was not recovered from the transcriptome dataset.

Table 3
Summary statistics of transcriptome assemblies generated for each species, including number of contigs (n), contiguity (N50), maximum contig length (max), total number of assembled base pairs (sum), and BUSCO scores: completeness (C %), single copy (S %), duplicate copies (D %), fragmented (F %) and missing (M %), compared to the total number (2,934) of arachnida_odb10 BUSCOs searched, as well as the number of putative visual opsins (Vis Ops) and total opsins (Total Ops) identified from each transcriptome.

Family	Species	n	N50 (bp)	Max (bp)	Sum (Mbp)	C %	S %	D %	F %	M %	Vis Ops	Total Ops
Salticidae	*Hasarius adansoni*	73,887	2,139	28,777	597	95.8	88.7	7.1	0.6	3.6	4	8
	Habrocestum africanum	80,990	2,115	41,404	589	97.4	90.5	6.9	0.4	2.2	3	7
	Menemerus bivittatus	66,240	2,334	45,746	592	97.1	90.2	6.9	0.6	2.3	3	7
Lycosidae	*Pardosa pseudoannulata*	45,677	1,569	37,427	267	81.4	77.8	3.6	6.3	12.3	3	5
	Schizocosa rovneri	38,960	2,310	23,615	384	92.3	87.2	5.1	1.3	6.4	4	5

3.2. Primary eyes - AMEs

Ultraviolet-green (UV-G) dichromacy has been widely documented in salticid AMEs (De Voe, 1975; Blest, 1985a; Blest, 1985b), which, when combined with the unique boomerang shape of the retina and photoreceptor layering, provides depth perception via chromatic-aberration-based image defocus (Land 1969b; Eakin and Brandenburger, 1971; Williams and McIntyre, 1980; Nagata et al., 2012). Our data support previous studies of opsin protein localization in the AMEs (Nagata et al., 2012; Terakita and Nagata, 2014), with RH1 segregated

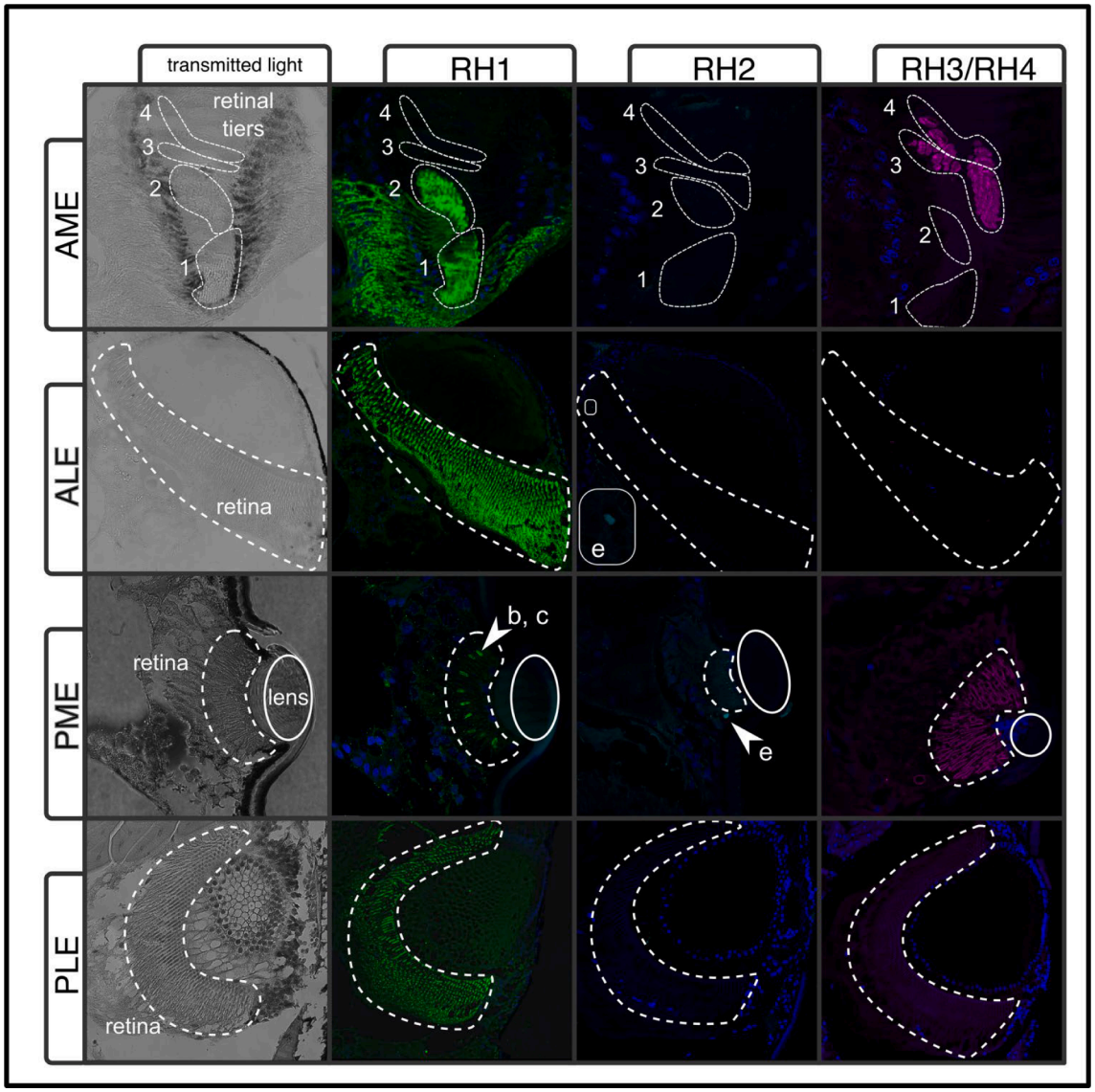

Fig. 3. *Hasarius adansoni* immunohistological images generated from confocal Leica microscope TCS SP8 using a 63x lens for median eyes and a 20x lens for lateral eyes. Images for eye types are organized in rows (i.e. AMEs, ALEs, PMEs, PLEs), with representative images for each eye type organized in columns for transmitted light images followed by each antibody used (i.e. RH1 in green, RH2 in cyan, RH3/RH4 in magenta; DAPI nuclei staining in blue in all confocal images). For anatomical orientation, retinal tiers in the AMEs and retinas in the secondary eyes are outlined in dashed lines; lenses are outlined with a solid line for the PMEs. Unique labeling patterns as outlined in Fig. 1 are annotated with arrows to indicate dispersed (b) and reduced (c) photoreceptors and proximal cells (e). (For interpretation of the references to color in this figure legend, the reader is referred to the web version of this article.)

in the proximal tiers 1 and 2, and RH3 in the distal tiers 3 and 4 for all three species (Fig. 1; Nagata et al., 2012). Our findings agree with UV-G dichromacy for both *H. adansoni* (Fig. 3) and *H. africanum* (Fig. 4). The RH2 opsin localized in all tiers of *M. bivittatus* AMEs (Fig. 5), which confirmed the predicted presence of *Rh2* from our RT-PCR on individually dissected eyes (Fig. S1). Electrophysiological measurements of the closely related species *Menemerus confusus* suggested four photoreceptor types (UV, blue, green, and yellow) for tetrachromatic vision (Yamashita and Tateda, 1976). The localization of the RH2 opsin in *M. bivittatus* may provide a mechanism for blue sensitivity and suggests expanded color vision may be common across the genus, but leaves open the question of how yellow sensitivity is achieved in *M. confusus*. To better understand the potential for an expanded set of color sensitivities in *M. bivittatus,* additional studies are needed, including investigations of the arrangement in each tier of the RH1-, RH2-, and RH3-based visual pigments to investigate whether photoreceptors express the same opsins, express different opsins, or are co-expressing sets of these opsins.

3.3. Secondary eyes – ALEs, PLEs, PMEs

Our opsin protein localization patterns demonstrate extreme variation in the distribution of opsins across the retinas of secondary eyes within as well as among species, a surprising find considering most previous literature suggested uniform structure and spectral sensitivity of these eyes (Eakin and Brandenburger, 1971; Yamashita and Tateda, 1976; Duelli, 1978; Hardie and Duelli, 1978; Land, 1985; Blest, 1987). These patterns also highlight variations in photoreceptor structural arrangements, with some secondary eyes having tiered or reduced labeling patterns (Fig. 1). These differences in opsin localization and photoreceptor arrangements imply differences in overall spectral sensitivities and the potential for color detection in each secondary eye type, which are further elucidated below.

The lateral eyes (ALEs and PLEs): The expected spectral sensitivity of jumping spider lateral eyes is in the 'green' portion of the visible spectrum (e.g. ~ 500–570 nm) based on limited ERG measurements in

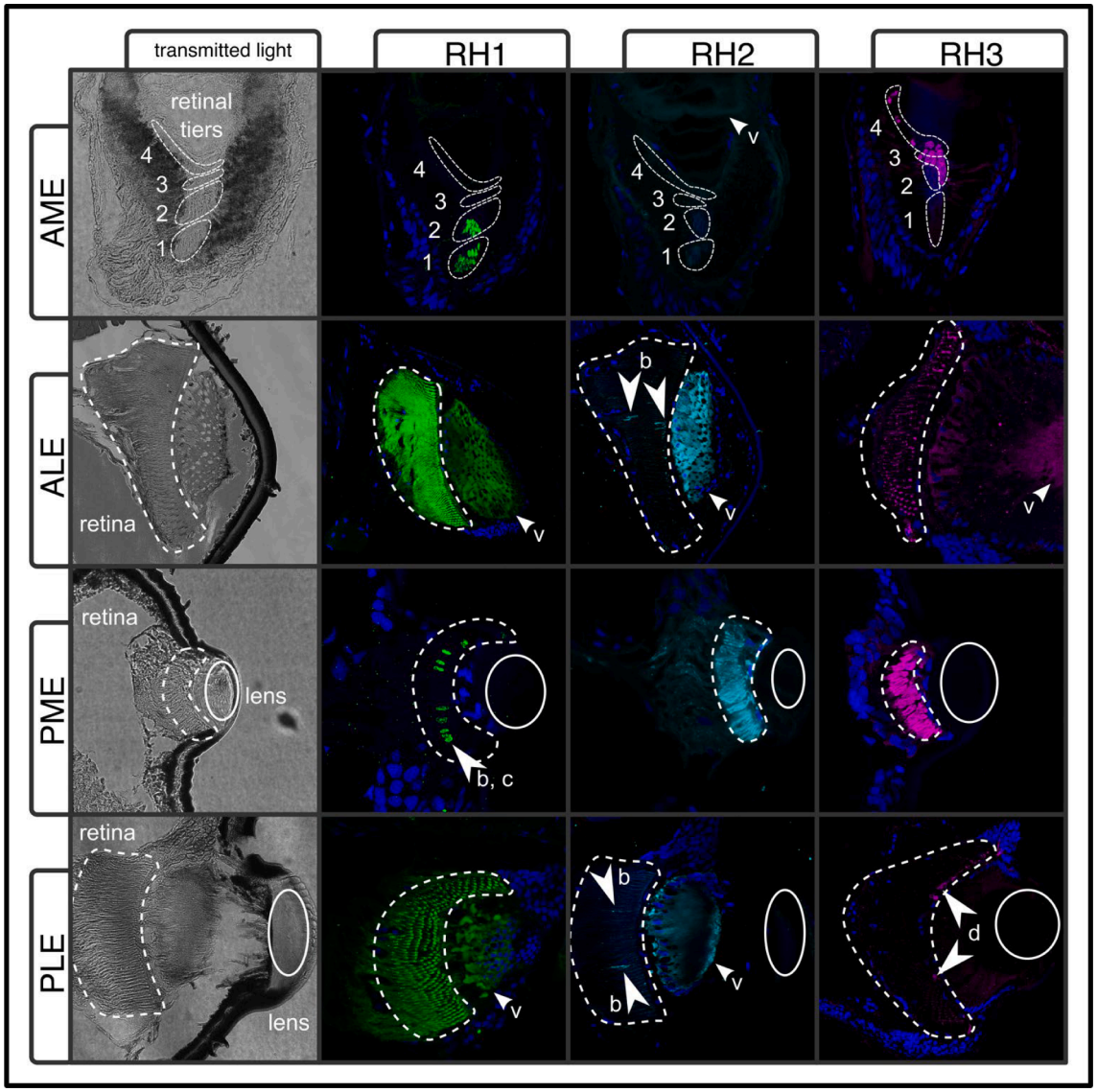

Fig. 4. *Habrocestum africanum* immunohistological images generated from confocal Leica microscope TCS SP8 using a 63x lens for median eyes and a 20x lens for lateral eyes. Images for eye types are organized in rows (i.e. AMEs, ALEs, PMEs, PLEs), with representative images for each eye type organized in columns for transmitted light images followed by each antibody used (i.e. RH1 in green, RH2 in cyan, RH3 in magenta; DAPI nuclei staining in blue in all confocal images). For anatomical orientation, retinal tiers in the AMEs and retinas in the secondary eyes are outlined in dashed lines; lenses are outlined with a solid line for the posterior eyes (i.e. PMEs and PLEs). Arrows indicate labeling patterns as outlined in Fig. 1 for dispersed photoreceptors (b), reduced photoreceptors (c), distal photoreceptors (d), or vitreous cells (v). (For interpretation of the references to color in this figure legend, the reader is referred to the web version of this article.)

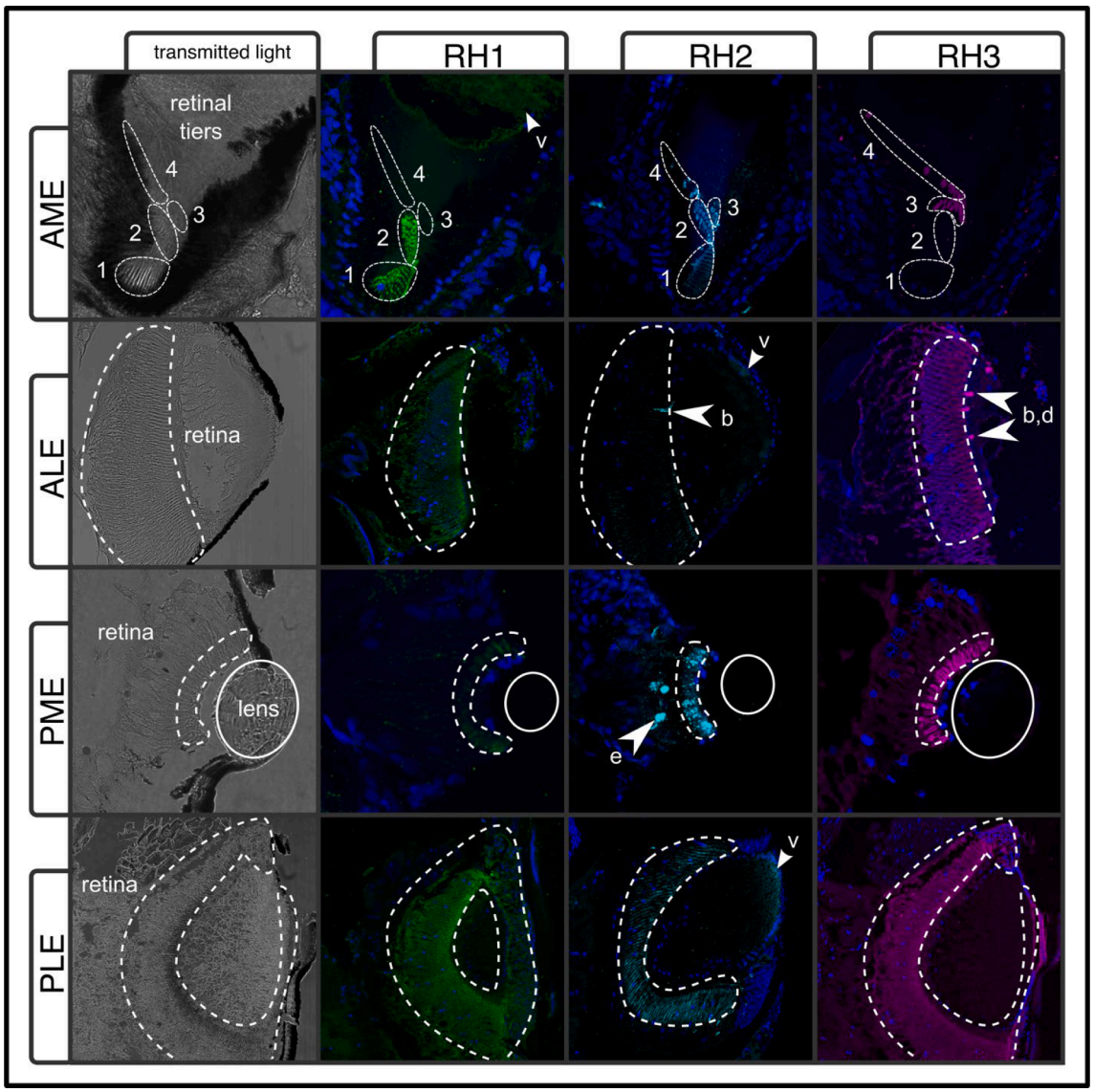

Fig. 5. *Menemerus bivittatus* immunohistological images generated from confocal Leica microscope TCS SP8 using a 63x lens for median eyes and a 20x lens for lateral eyes. Images for eye types are organized in rows (i.e. AMEs, ALEs, PMEs, PLEs), with representative images for each eye type organized in columns for transmitted light images followed by confocal images of each antibody used (i.e. RH1 in green, RH2 in cyan, RH3 in magenta; DAPI nuclei staining in blue in all confocal images). For anatomical orientation, retinal tiers in the AMEs and retinas in the secondary eyes are outlined in dashed lines; lenses are outlined with a solid line for the PMEs. Labeling patterns as outlined in Fig. 1 are indicated by arrows for dispersed photoreceptors (b), distal photoreceptors (d), proximal cells (e), and vitreous cells (v). (For interpretation of the references to color in this figure legend, the reader is referred to the web version of this article.)

Menemerus confusus (536 nm in ALEs and PLEs; Yamashita and Tateda, 1976) and *Plexippus validus* (535 nm in PLEs; Hardie and Duelli, 1978), matching the molecular studies of the putatively green-sensitive RH1 opsin localization in *H. adansoni* (Koyanagi et al., 2008; Nagata et al., 2012; Terakita and Nagata, 2014). While we confirmed that RH1 is the predominant opsin across most lateral eye retinas of the three species investigated here, it was not the only opsin localized in either the ALEs or the PLEs. The forward-facing ALEs had unique RH2 and RH3 opsin patterns in each species. *H. adansoni* did not localize RH2 nor RH3 within the photoreceptors of the retina (Figs. 1, 3). In *H. africanum*, RH2 was found in only a few photoreceptors while RH3 was localized more broadly, suggesting a complex retinal mosaic of photoreceptors (Figs. 1, 4). In *M. bivittatus*, RH2 was located in only a few photoreceptors while RH3 was dispersed as either isolated distal cells or within all retinal photoreceptors (Figs. 1, 5).

The PLEs were equally diverse in opsin localizations. In *H. adansoni,* past studies suggested that *Rh1*, *Rh2* and *Rh4* (the *H. adansoni*-specific *Rh3* duplicate) were transcribed in the PLE retina, with *Rh2 in situ* probes labeling only a single photoreceptor (Nagata et al., 2012). In contrast, in this study only RH1 was found in *H. adansoni* PLE photoreceptors, instead matching our ALE patterns (Figs. 1, 3; Table 1). *H. africanum* PLEs had RH2 dispersed in only a few PLE photoreceptors per section while the RH3 opsin was restricted to the distal portion of the entire retina (Figs. 1, 4). In *M. bivittatus* PLEs all three opsins were uniformly distributed in photoreceptors across the entire retina (Figs. 1, 5).

The lateral eyes in the three study species displayed an unexpected diversity of opsins and photoreceptor arrangements, particularly with respect to the dispersed and/or tiered arrangements of photoreceptors containing RH2 or RH3. The distal distribution of RH3 proteins in the PLE of *H. africanum* and the ALE of *M. bivittatus* suggests several anatomical possibilities. The first is that the lateral eyes of some species contain stacked or layered photoreceptors, with a distal short-wavelength-sensitive photoreceptor tier and proximal longer-wavelength-sensitive photreceptor tier. While stacked or layered

receptors have not previously been observed in salticid secondary eyes, our results point to a UV-sensitive RH3-based visual pigment distal to the longer wavelength-based receptors (RH1 and/or RH2), an arrangement similar to that of arthropod rhabdoms in compound eyes (e.g., crab spiders – O'Carroll, 1989; mysid shrimp – Hallberg, 1977; stomatopods – Schönenberger, 1977; isopods – Nilsson, 1978; decapods – Eguchi, 1965; damselflies – Ninomiya et al., 1969). Interestingly, the distal RH3 cells were localized in different patterns between species and lateral eyes. In the *M. bivittatus* ALE retinas, the distal RH3 cells were distributed and it was unclear whether they sat atop RH1 receptors, RH2 receptors, both, or neither. In *H. africanum*, distal RH3 cells were located across the entire PLE retina, likely atop both RH1 and RH2 receptors. Alternatively, the location of the RH3 signal is similar to the expected anatomical structure of photoreceptor soma or the associated support cells of a retinal mosaic, rather than rhabdoms, possibly indicating that these visual pigments may be acting as a spectral filter due to their orientation in the light path above the retina (Blest, 1985a; Blest, 1985b). Detailed histological and electrophysiological studies of the lateral eye retinas are needed to distinguish between these two possibilities. The anatomical structure of the lateral eyes has only been investigated in a few species; both pairs of eyes were observed to have a regular array of paired rhabdomeres per photoreceptor (Eakin & Brandenburger, 1971; Duelli, 1978; Blest, 1985a; Blest, 1985b). In this study we were unable to distinguish whether or not the patterns of the opsin localization across the retinal mosaics were co-localized within the same photoreceptor cell. While co-localization within a single photoreceptor has been observed in other arthropods (e.g., butterflies – Arikawa et al., 2003; flour beetles - Jackowska et al., 2007; decapod crabs - Rajkumar et al., 2010; horseshoe crabs - Katti et al., 2010, Battelle et al., 2016), it has yet to be documented in spiders.

The posterior median eyes (PMEs): The final eye type, the PME, was expected to be the most rudimentary of the eyes based on past anatomical studies. In most salticids in the clade Saltafresia (our species included), the PMEs are reduced in size compared to more basal salticid lineages, and the retina is so small in the few species studied that the PMEs are thought to be largely vestigial (Blest, 1983; Land, 1985). Despite this, previous studies found both RH2 (blue-sensitive) and RH4 (UV-sensitive) opsins across the entire PME retina of *H. adansoni* (Nagata et al., 2012; Terakita and Nagata, 2014), suggesting the potential for color vision. Even more surprising, the variation observed in the labeling patterns for this eye were the highest among all of the eye types, suggesting not only functional relevance to jumping spider vision, but that PME spectral function varies across species and may be linked to distinct ecological features or visual behaviors.

In contrast to the lateral secondary eyes (ALEs and PLEs), where retinas were dominated by RH1 opsins, the PMEs in all species had RH3/RH4 opsins localized across the entire retina with variation in the number and arrangement of cells localizing RH1 and RH2 opsins (Figs. 1, 3-5). Our RH3-antibody labeled the entire *H. adansoni* PME retina, confirming previously reported *Rh4* RT-PCR results (Nagata et al., 2012), as our antibody does not differentiate between the *H. adansoni* RH3 and RH4 opsins (Table 1). In *H. adansoni* we were unable to replicate RH2 labeling across the entire retina, as documented with *in situ* hybridization and immunohistochemistry in previous studies (Nagata et al., 2012; Terakita and Nagata, 2014). Instead, we found that in the *H. adansoni* PMEs, RH1 labeled small distributed cells reduced in size, resulting in a more punctate labeling pattern; due to limited study of this particular eye in salticids it is unclear whether these are photoreceptive cells or support cells (Figs. 1, 3). RH1 was also localized in smaller distributed retinal cells in the *H. africanum* PMEs, but RH2 localized to photoreceptor cells across the entire retina (Figs. 1, 4). Finally, RH1 and RH2 localized across the entire retina in *M. bivittatus* PME retinas (Figs. 1, 5).

When taken all together, the varied opsin distribution patterns from different species suggests that PMEs are not vestigial and indeed have functions strongly tied to ecological light environment. Although the size and position on the cephalothorax varies among salticid species, the PMEs are generally the most dorsally positioned salticid eyes and therefore the pair of eyes most perpetually directed skyward. Given the low resolution of PMEs, the retinal dominance of the short-wavelength sensitive opsins RH2 and RH3 could be used for increased sensitivity to dark looming stimuli on a brightly skylit background for predator avoidance. Alternatively, this eye is reminiscent of insect ocelli, both in the skyward orientation and arrangement of the lens relative to the retina leading to under-focused images (Cornwell, 1955). The ocelli in many flying insects function as horizon detectors for animals rapidly moving in three dimensions (Stange et al., 2002). Jumping spider PMEs similarly may be essential horizon detectors for these animals as they rapidly jump through space or estimate their position when navigating complex habitat structures. Much like studies across insect taxa that revealed diverse ocellar visual capabilities (Hung and Ibbotson, 2014), our results suggest PME function across salticid species is highly variable. Most insect ocelli characterized, however, have documented green and UV sensitivity (Henze et al., 2012). The variability in PME opsin localization among species, particularly the dominance of RH2 (blue-sensitive) and RH3 (UV-sensitive) receptors, may reflect the specific ecologies of each species with respect to what constitutes the 'horizon' in different microhabitats (e.g., foliage and leaf litter - *H. adansoni*; rock walls and tree trunks - *M. bivittatus*; leaf litter in savanna habitats - *H. africanum*).

3.4. Notable non-retinal labeling

Expression levels of each opsin transcript (Fig. 2) suggested *Rh2* was more prevalent in the cephalothorax than our retinal labeling would explain, particularly for *H. adansoni*. Likely, this indicates the RH2 opsin is involved in non-ocular light detection, and indeed a few notable localizations confirmed this was the case.

Contrary to previous research, we do not report RH2 localization in the retina of *H. adansoni* PMEs. The only RH2 localization we observed in *H. adansoni* was in isolated cells just outside of and below the photoreceptors in both the ALE and PME (Figs. 1, 3). We also observed these cells more obviously in *M. bivittatus* (Fig. 5). These isolated cells are likely located in neural tissue for the PMEs, suggesting that RH2 also has a non-visual function; a similar extra-retinal structure expressing synapsin was found in the PLEs of the salticid *Marpissina muscosa* (Steinhoff et al., 2020). One explanation for why we did not find this pattern in *H. africanum* is that we simply did not image enough sections to find this small, localized tissue. For example, only a single section from one ALE in one individual *H. adansoni* resulted in this pattern (Fig. 3). Alternatively, if we combine our results for RH2 with previous findings (Terakita and Nagata, 2014), a potential association emerges between rearing light environment and RH2 localization in cells outside the retina. All of our *M. bivittatus* and *H. adansoni* specimens, where cells proximal to the retina labeled with RH2, were wild caught and fixed within 2–12 h, while our *H. africanum* individuals and previously published results from *H. adansoni* individuals were lab reared for 3–6 months prior to fixation potentially resulting in RH2 expression across the entire retina of *H. adansoni*. The photoreceptors of salticids are expected to shed and degrade their rhabdoms during transitions between light and dark (i.e. dusk and dawn) to assist in sensitivity changes by modifying rhabdom size (Blest & Maples, 1979; Blest, 1985a; Blest, 1985b). Therefore the variation in RH2 localization among species observed in the PMEs may pertain to the light environment of the animal the day of sacrifice and also implies that salticid eyes may dynamically alter opsin expression on experimentally relevant timescales. Most likely, a combination of both sections surveyed and rearing light environment influenced our results and more studies are needed to investigate these possibilities.

Perhaps related to the time of animal sacrifice relative to the shedding of opsin-containing membranes, another puzzling non-retinal label was observed in all three species investigated: opsin localization to the

vitreous layer above the retina. In *H. africanum*, RH2 localized to the vitreous layer in all eyes, RH1 to the vitreous of the lateral eyes (ALEs, PLEs), and RH3 to the ALE vitreous (Fig. 4). Vitreous labeling was weakly observed in *M. bivittatus* as well, though only for RH1 in the AMEs and RH2 in the lateral eyes (ALEs, PLEs) (Fig. 5). *H. adansoni* vitreous localization was even less than *M. bivittatus* with RH1 only weakly signaling in the lateral eyes (Fig. 3). At this point, beyond documenting opsin labeling in vitreous cells as a common pattern in jumping spider eyes, we can only speculate whether this pattern is the consequence of opsin shedding, of processes relating to the handling of specimens, or relevant in some other yet uncharacterized functional context (e.g., usage as a light filtering agent in the vitreous humor).

4. Summary

Our findings call into question previous assumptions about the uniformity of the secondary eyes in both spectral sensitivity and photoreceptor anatomical arrangements. By characterizing the full complement of visual opsins across all eye types, we have highlighted previously uncharacterized diversity in visual anatomy and function, particularly within the secondary eyes. Unexpectedly, we found diverse photoreceptor arrangements in secondary eyes suggesting the potential for retinal tiering and color vision, despite the low resolution of these eye types. One mechanism for color perception in these eyes would be neural comparison of the inputs from the putatively stacked photoreceptors in the lateral pairs of eyes in two species (*H. africanum* and *M. bivittatus*), a common photoreceptor arrangement in arthropods but novel in salticid secondary eyes. Further, our findings in the PME retinas lead to broader questions about the function of these tiny eyes, as all three opsins localized to these retinas in all species, albeit in species-specific patterns. While we are unable to establish the functional implications of these localization patterns based on our current results, one thing is certain: opsin expression of *Rh1* and *Rh3* is somewhat conserved within secondary eyes, between individuals, and among species, but *Rh2* expression varies highly in all contexts.

Here we have presented opsin localization patterns across all eye types in only three species of salticid, and all three exhibited marked variation in opsin localization both between eye types within a species and within eye types among taxa. The immense diversity in opsin localization characterized in this study may be attributed to the very different ecologies of these three species - *H. adansoni* is primarily a leaf litter, forest dweller with limited light exposure; *H. africanum* resides in brightly lit, open terrain; *M. bivittatus* commonly inhabits vertical walls and tree trunks. The visual ecologies of these three species represent a mere fraction of the ecological variation observed within the salticids overall. Given that each pair of eyes is likely involved in distinct visual tasks, and that the divergent light environments, hunting strategies, modes of conspecific identification, and predator avoidance strategies will influence what the visual systems of each species are attuned to, we predict even more variation across salticid species in photoreceptor arrangements, color detection capabilities, and lineages with expanded spectral sensitivities in their secondary eyes. While these eyes may be secondary, they should no longer be considered subordinate to the principal eyes.

CRediT authorship contribution statement

Mireille Steck: Writing – review & editing, Writing – original draft, Visualization, Investigation, Formal analysis, Data curation, Conceptualization. **Sophia J. Hanscom:** Writing – review & editing, Writing – original draft, Validation, Investigation. **Tom Iwanicki:** Writing – review & editing, Writing – original draft, Validation, Investigation. **Jenny Y. Sung:** Writing – review & editing, Investigation, Data curation. **David Outomuro:** Writing – review & editing, Resources, Investigation. **Nathan I. Morehouse:** Writing – review & editing, Resources, Funding acquisition, Conceptualization. **Megan L. Porter:** Writing – review & editing, Writing – original draft, Resources, Project administration, Funding acquisition, Conceptualization.

Declaration of competing interest

The authors declare that they have no known competing financial interests or personal relationships that could have appeared to influence the work reported in this paper.

Data availability

Sequence data have been deposited in NCBI's SRA database. Supporting data are available upon request: alignment files, newick tree files, raw and processed confocal images.

Acknowledgements

Collection and preservation of specimens from Africa would not have been possible without the help of Charles Haddad (University of the Free State), Kiran Marathe (University of British Columbia), and Josh Gross (University of Cincinnati). Specimens collected locally were made possible by Olivia Harris (University of Cincinnati), Wayne Maddison (University of British Columbia), and Kristianne Agusto. Animal histology would have been subpar without the ingenuity and patience of Miyoko Bellinger at the Histopathology Core at the John A. Burns School of Medicine. Images acquired from the Biological Electron Microscope Facility at the Pacific Biosciences Research Center were made possible by the fantastic invertebrate enthusiast Tina Carvalho. This work was funded by the National Science Foundation [IOS-1831749 to MLP; IOS-1831767 to NIM]. Computing resources used for transcriptome assembly were supported by the National Science Foundation under grant nos. DBI-1062432 2011, ABI-1458641, and ABI-1759906 2018 to Indiana University as well as Lilly Endowment Inc. through its support for the Indiana University Pervasive Technology Institute. Research reported in this publication was supported by the National Institute of General Medical Sciences of the National Institutes of Health under Award Number P20GM125508, the National Institute on Minority Health and Health Disparities of the National Institutes of Health, and Ola Hawai'i under award number U54MD007601. The content is solely the responsibility of the authors and does not necessarily represent the official views of the National Institutes of Health. This is publication #217 from the School of Life Sciences, University of Hawai'i at Mānoa.

Appendix A. Supplementary data

Supplementary data to this article can be found online at https://doi.org/10.1016/j.visres.2024.108367.

References

Arikawa, K., Mizuno, S., Kinoshita, M., et al. (2003). Coexpression of two visual pigments in a photoreceptor causes an abnormally broad spectral sensitivity in the eye of the butterfly *Papilio xuthus*. *Journal of Neuroscience, 23*, 4527–4532.

Battelle, B.-A., Ryan, J. F., Kempler, K. E., et al. (2016). Opsin repertoire and expression patterns in horseshoe crabs: Evidence from the genome of Limulus polyphemus (Arthropoda: Chelicerata). *Genome Biol Evol, 8*, 1571–1589. https://doi.org/10.1093/gbe/evw100

Bednarski, J., Taylor, P., & Jakob, E. M. (2012). Optical cues used in predation by jumping spiders, Phidippus audax (Araneae, Salticidae). *Animal Behaviour, 84*, 1221–1227.

Blest, A. D. (1983). Ultrastructure of Secondary Retinae of Primitive and Advanced Jumping Spiders (Araneae, Salticidae). *Zoomorphology, 102*, 125–141.

Blest, A. D. (1985a). V. The fine structure of spider photoreceptors in relation to function. In *Neurobiology of arachnids* (pp. 79–102). Berlin, Heidelberg: Springer-Verlag.

Blest, A. D. (1985b). Retinal mosaics of the principal eyes of jumping spiders (Salticidae) in some neotropical habitats: Optical trade-offs between sizes and habitat illuminances. *Journal of Comparative Physiology A, 157*, 391–404.

Blest, A. D. (1987). The retinae of *Euryattus bleekeri*, an aberrant salticid spider from Queensland. *J Zool, 211*, 399–408.

Blest, A. D., Hardie, R. C., McIntyre, P., & Williams, D. (1981). The spectral sensitivities of identified receptors and the function of retinal tiering in the principal eyes of jumping spiders. *J Comp Physiol A, 145*, 227–239.

Blest, A. D., & Maples, J. (1979). Exocytotic shedding and glial uptake of photoreceptor membrane by a salticid spider. *Proc R Soc Lond B, 204*, 105–112. https://doi.org/10.1098/rspb.1979.0016

Blest, A. D., O'Carroll, D. C., & Carter, M. (1990). Comparative ultrastructure of Layer I receptor mosaics in principal eyes of jumping spiders: The evolution of regular arrays of light guides. *Cell Tissue Res, 262*, 445–460.

Blest, A. D., & Price, G. D. (1984). Retinal mosaics of the principal eyes of some jumping spiders (Salticidae: Araneae): Adaptations for high visual acuity. *Protoplasma, 120*, 172–184.

Blest, A. D., & Sigmund, C. (1984). Retinal mosaics of the principal eyes of two primitive jumping spiders, Yaqinumanis and Lyssomanes: Clues to the evolution of Salticid vision. *Proc R Soc Lond B, 221*, 111–125.

Cerveira, A. M., Jackson, R. R., & Nelson, X. J. (2019). Dim-light vision in jumping spiders (Araneae, Salticidae): Identification of prey and rivals. *Journal of Experimental Biology, 222*, jeb198069.

Cornwell, P. (1955). The functions of the ocelli of Calliphora (Diptera) and Locusta (Orthoptera). *Journal of Experimental Biology, 32*, 217–237.

De Voe, R. D. (1975). Ultraviolet and green receptors in principal eyes of jumping spiders. *J Gen Physiol, 66*, 193–207.

Dolev, Y. (2016). *Visual perception in jumping spiders (Araneae*. Salticidae): University of Canterbury.

Duelli, P. (1978). Movement detection in the posterolateral eyes of jumping spiders (Evarcha arcuata, Salticidae). *Journal of Comparative Physiology, 124*, 15–26.

Eakin, R. M., & Brandenburger, J. L. (1971). Fine structure of the eyes of jumping spiders. *Journal of Ultrastructure Research, 37*, 618–663.

Eguchi, E. (1965). Rhabdom structure and receptor potentials in single crayfish retinular cells. *Journal of Cellular and Comparative Physiology, 66*, 411–429.

Foelix, R. F. (2011). *Biology of Spiders* (3rd edn.). United Kingdom: Oxford University Press.

Gilbert, D. G. (2019). Longest protein, longest transcript or most expression, for accurate gene reconstruction of transcriptomes? *BioRxiv*, 829184.

Glenszczyk, M., Outomuro, D., Gregorič, M., et al. (2022). The jumping spider *Saitis barbipes* lacks a red photoreceptor to see its own sexually dimorphic red coloration. *Sci Nat, 109*, 6. https://doi.org/10.1007/s00114-021-01774-6

Grabherr, M. G., Haas, B. J., Yassour, M., et al. (2011). Full-length transcriptome assembly from RNA-Seq data without a reference genome. *Nature biotechnology, 29*, 644–652.

Gühmann, M., Porter, M. L., & Bok, M. J. (2022). The Gluopsins: Opsins without the Retinal Binding Lysine. *Cells, 11*, 2441.

Hallberg, E. (1977). The fine structure of the compound eyes of mysids (Crustacea: Mysidacea). *Cell Tissue Res, 184*, 45–65.

Hardie, R. C., & Duelli, P. (1978). Properties of single cells in posterior lateral eyes of jumping spiders. *Zeitschrift für Naturforschung C, 33*, 156–158.

Harland, D. P. (2000). *Optical cues and vision-based discrimination mechanisms underlying predatory versatility in jumping spiders (Araneae: Salticidae)*. Doctor of Philosophy in Zoology, University of Canterbury.

Henze, M. J., Dannenhauer, K., Kohler, M., et al. (2012). Opsin evolution and expression in arthropod compound eyes and ocelli: Insights from the cricket *Gryllus bimaculatus*. *BMC evolutionary biology, 12*, 1–16.

Hill, D. E., & Richman, D. B. (2009). The evolution of jumping spiders (Aranea: Salticidae): A review. *Peckhamia, 75*, 1–7.

Hung, Y.-S., & Ibbotson, M. R. (2014). Ocellar structure and neural innervation in the honeybee. *Frontiers in Neuroanatomy, 8*.

Jackowska, M., Bao, R., Liu, Z., et al. (2007). Genomic and gene regulatory signatures of cryptozoic adaptation: Loss of blue sensitive photoreceptors through expansion of long wavelength-opsin expression in the red flour beetle *Tribolium castaneum*. *Frontiers in zoology, 4*, 1–11.

Jakob, E. M., Long, S. M., Harland, D. P., et al. (2018). Lateral eyes direct principal eyes as jumping spiders track objects. *Current Biology, 28*, R1092–R1093.

Katoh, K., Misawa, K., Kuma, K., & Miyata, T. (2002). MAFFT: A novel method for rapid multiple sequence alignment based on fast Fourier transform. *Nucleic acids research, 30*, 3059–3066.

Katoh, K., & Standley, D. M. (2013). MAFFT multiple sequence alignment software version 7: Improvements in performance and usability. *Molecular biology and evolution, 30*, 772–780.

Katti, C., Kempler, K., Porter, M., et al. (2010). Opsin co-expression in Limulus photoreceptors: Differential regulation by light and a circadian clock. *Journal of Experimental Biology, 213*, 2589–2601.

Koyanagi, M., Nagata, T., Katoh, K., et al. (2008). Molecular evolution of arthropod color vision deduced from multiple opsin genes of jumping spiders. *Journal of Molecular Evolution, 66*, 130–137.

Land, M. F. (1969a). Movements of the retinae of jumping spiders (Salticidae: Dendryphantinae) in response to visual stimuli. *Journal of Experimental Biology, 51*, 471–493.

Land, M. F. (1969b). Structure of the retinae of the principal eyes of jumping spiders (Salticidae: Dendryphantinae) in relation to visual optics. *Journal of Experimental Biology, 51*, 443–470.

Land, M. F. (1985). The morphology and optics of spider eyes. In *Neurobiology of arachnids* (pp. 53–78). Berlin Heidelberg, Berlin, Heidelberg: Springer.

Manni, M., Berkeley, M. R., Seppey, M., et al. (2021). BUSCO update: Novel and streamlined workflows along with broader and deeper phylogenetic coverage for scoring of eukaryotic, prokaryotic, and viral genomes. *Molecular biology and evolution, 38*, 4647–4654.

Morehouse, N. I. (2020). Spider Vision. *Current Biology, 30*, R975–R980.

Morehouse, N. I., Buschbeck, E. K., Zurek, D. B., et al. (2017). Molecular Evolution of Spider Vision: New Opportunities, Familiar Players. *Biol Bull, 233*, 21–38.

Nagata, T., Koyanagi, M., Tsukamoto, H., et al. (2012). Depth Perception from Image Defocus in a Jumping Spider. *Science, 335*, 469–471. https://doi.org/10.1126/science.1211667

Nilsson, H. L. (1978). The fine structure of the compound eyes of shallow-water Asellotes, Jaera albifrons Leach and Asellus aquaticus L. (Crustacea: Isopoda). *Acta Zoologica, 59*, 69–84.

Ninomiya, N., Tominaga, Y., & Kuwabara, M. (1969). The fine structure of the compound eye of a damsel-fly. *Zeitschrift für Zellforschung und Mikroskopische Anatomie, 98*, 17–32.

O'Carroll, D. (1989). *An optical assessment of visual performance in the eyes of hunting spiders (Araneae: Labidognatha)*. Diss Flinders Univ Aust.

Porter, M. L., Blasic, J. R., Bok, M. J., et al. (2012). Shedding new light on opsin evolution. *Proc R Soc B, 279*, 3–14. https://doi.org/10.1098/rspb.2011.1819

Rajkumar, P., Rollmann, S. M., Cook, T. A., & Layne, J. E. (2010). Molecular evidence for color discrimination in the Atlantic sand fiddler crab, *Uca pugilator*. *Journal of Experimental Biology, 213*, 4240–4248.

Rambaut, A. (2018). FigTree v1. 4.4, a Graphical Viewer of Phylogenetic Trees. 2014. Java.

Ramirez, M. D., Pairett, A. N., Pankey, M. S., et al. (2016). The last common ancestor of most bilaterian animals possessed at least nine opsins. *Genome biology and evolution, 8*, 3640–3652.

Richman, D. B., & Jackson, R. R. (1992). A review of the ethology of jumping spiders (Araneae, Salticidae). *Bulletin of the British Arachnological Society, 9*, 33–37.

Schönenberger, N. (1977). The fine structure of the compound eye of Squilla mantis (Crustacea, Stomatopoda). *Cell and Tissue Research, 176*, 205–233.

Spano, L., Long, S. M., & Jakob, E. M. (2012). Secondary eyes mediate the response to looming objects in jumping spiders (Phidippus audax, Salticidae). *Biology Letters, 8*, 949–951.

Stange, G., Stowe, S., Chahl, J., & Massaro, A. (2002). Anisotropic imaging in the dragonfly median ocellus: A matched filter for horizon detection. *Journal of Comparative Physiology A, 188*, 455–467.

Steinhoff, P. O. M., Uhl, G., Harzsch, S., & Sombke, A. (2020). Visual pathways in the brain of the jumping spider Marpissa muscosa. Journal of Comparative. *Neurobiology, 528:11. bioRxiv 640706*. https://doi.org/10.1101/640706

Terakita, A., & Nagata, T. (2014). Functional Properties of Opsins and their Contribution to Light-Sensing Physiology. *Zoological Science, 31*, 653–659. https://doi.org/10.2108/zs140094

Trifinopoulos, J., Nguyen, L.-T., von Haeseler, A., & Minh, B. Q. (2016). W-IQ-TREE: A fast online phylogenetic tool for maximum likelihood analysis. *Nucleic acids research, 44*, W232–W235.

Williams, D. S., & McIntyre, P. (1980). The principal eyes of a jumping spider have a telephoto component. *Nature, 288*, 578–580.

Winsor, A. M., Morehouse, N. I., & Jakob, E. M. (2023). Distributed Vision in Spiders. In *Distributed Vision: From Simple Sensors to Sophisticated Combination Eyes* (pp. 267–318). Cham: Springer.

Yamashita, S., & Tateda, H. (1976). Spectral sensitivities of jumping spider eyes. *J Comp Phys, 105*, 29–41.

Zurek, D. B., Cronin, T. W., Taylor, L. A., et al. (2015). Spectral filtering enables trichromatic vision in colorful jumping spiders. *Current Biology, 25*, R403–R404.

Zurek, D. B., Taylor, A. J., Evans, C. S., & Nelson, X. J. (2010). The role of the anterior lateral eyes in the vision-based behaviour of jumping spiders. *Journal of Experimental Biology, 213*, 2372–2378.